

# Lane data fusion for driver assistance systems

**Albrecht Klotz**

Robert Bosch GmbH  
Daimlerstraße 6,  
71229 Leonberg  
Germany

albrecht.klotz@de.bosch.com

**Jan Sparbert**

Robert Bosch GmbH  
Daimlerstraße 6  
71229 Leonberg  
Germany

jan.sparbert@de.bosch.com

**Dieter Hötzer**

Robert Bosch GmbH  
Daimlerstraße 6  
71229 Leonberg  
Germany

dieter.hoetzer@de.bosch.com

**Abstract** – The objective of the presented fusion algorithms is to supply driver assistance systems (DAS), e.g. an advanced adaptive cruise control (ACC), with one or more hypotheses of the possible lane layout in front of the own vehicle. Different sources of information are considered, namely line markings detected by a video-sensor, information derived from trajectories of moving objects and data from a digital map. These data sets are described and fused mathematically closed and consistent, widely independent of the DAS. The fusion algorithm relies on mathematical modelling taking the relative accuracy of the different sensor sources into account. Additionally, a priori and heuristic knowledge of the input data is used in creating hypotheses. The fused lane-data can be used in an ACC-system for a better prediction of the own vehicle's course. This allows a more robust and dynamical system application as well as predictive system intervention without the need of combining these data within the ACC-system itself.

**Keywords:** Driver assistance system, course prediction, lane data fusion, sensor data fusion.

## 1 Introduction

Driver assistance systems like adaptive cruise control (ACC) have been successfully introduced into the market since several years. The currently available ACC systems are based on single surround sensor technologies (either Radar or LIDAR) [1] and are dedicated to a restricted area of operation, e.g. well structured road geometries like motorways. Target object selection is based on the own vehicle course prediction derived from the vehicle yaw rate and sometimes on evaluation of collective motion of other vehicles. Future ACC systems will expand the regime of operation to more complex road scenarios like “curvy” highways (with curve radii below 100m) or even to urban environments. They try to deal with situations currently hard to handle like stable follow mode on exits of motorways or at entries of sharp curves. These environments pose higher requirements to the accuracy of the course prediction to allow a controlled and transparent ACC functionality. Predictive approaches for course estimation solemnly based on the yaw rate seem not sufficient for this task. Therefore, one major objective for future ACC systems is to provide the ACC function with one or more course hypotheses of the potential course of the ego vehicle by fusing all available “course-like” or “lane-like” data and provide information about the lane

layout in a mathematically closed and consistent way. It also does not seem sufficient to add only a video based lane detection system since the required look ahead distances are hard to achieve with low-cost video systems and lane markings are not available all the time.

Besides improved course prediction several other benefits for an ACC system may be subsequently obtained e.g. more robust and faster cut-in/cut-out detection and suppression of false alarms. In addition benefits are also expected for automotive safety systems like automatic emergency brake.

### 1.1 Concepts of lane data fusion

In this paper two approaches for lane data fusion (LDF) are discussed and first results are presented: a coefficient based fusion approach and a fusion scheme in spatial coordinates. Alternative approaches have also been discussed in literature [2].

The LDF is one major building block in an information platform comprising object-, line- and vehicle data fusion.

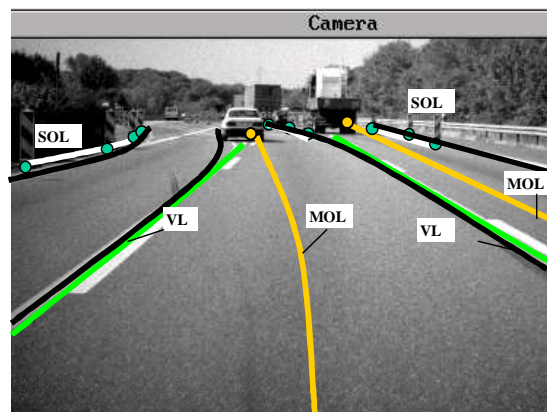


Fig. 1: Scenario with moving object lines (MOL), video line markings (VL), data from stationary objects (SOL) and fusion lanes (black) (displayed data not measured). NDM data not shown.

In the following the word “ego” will refer to the own vehicle. The word “line” will be referred to as being the basic input data for the fusion algorithms representing any considered component of the lane layout. Lines could either be road markings detected by a video sensor (VL)

[3], trajectory-lines calculated by moving objects (MOL), road (line) boundary information estimated by stationary objects (SOL, not considered in this paper) [4] or road layout information extracted from a digital map (NDM). The approach shall in general be able to deal with all combinations of line input data. Fig. 1 sketches a typically scenario indicating the idea of LDF.

## 2 Fusion of coefficients

### 2.1 General approach

In the first approach a LDF of the coefficients of a polynomial model is performed. A lane consists of two parallel shifted lines represented by

$$y_{l,r} = f(x) = y_{Start} \pm \frac{b}{2} + \tan(\psi)x + \frac{1}{2}c_0x^2 + \frac{1}{6}c_1x^3 \quad (1)$$

in the ego vehicle coordinate system with x in driving direction and y positive to the left, see for example [5]. The coefficients are: lateral shift of the lanes  $y_{Start}$  at  $dx_{Start}$ , the width of the lane  $b$ , the angle  $\psi$  of ego vehicle relatively to the line at  $dx_{Start}$ , the curvature  $c_0$ , and curvature derivative  $c_1$ . Lanes are allowed to overlap like crossings of a railway.

The algorithm for the LDF with coefficients can be implemented very efficiently. However, it may become erroneous or less robust if the order of the model gets higher and coefficients are estimated completely independently of the different line sources. Therefore, for the estimation of the lines similar models are applied in the vision sensor and the trajectory estimator and constraints for the  $\psi$ ,  $y_{Start}$  and  $c_1$  parameters are applied.

The fusion algorithm consist of the steps shown in Fig. 2.



Fig. 2: Major steps of the coefficient fusion algorithm.

At the beginning of a cycle, the coefficients of the fusion lanes of the last cycle are predicted to compensate the ego vehicle motion. Currently, a first order approximation is adequate.

In the next step a split of the lane into two parallel shifted lines is carried out. If the curvature coefficients are large, they are post-processed in order to account for the differences in curvature for the inner and outer line in a curve.

Thereafter, fusion lines with quite similar coefficients are merged. Merging happens, if a line contributes to two neighboring lanes and so appears twice after the split.

Then, the main part of the fusion starts with the association of sensor input lines to fusion lines. Here, a gate association in coefficient space with some

modifications is used. The method will be described in section 2.2. It's mentioned, that the same association routine is used three times: for the merging (association of fusion lines), for the sensor line to fusion line association, and for lane building (association of fusion lines with knowledge of the lane's width). For each case a different parameter set is used.

In the following step the coefficients of all sensor lines associated to a fusion line are averaged to a resulting pre-fusion line using a weighted mean. The weights are chosen according to the a priori knowledge of the relative accuracy of the coefficient of the different line sources. The same routine is used again later in the lane-fusion.

The lane building process is quite similar to the pre-fusion of sensor lines. First, the resulting pre-fusion lines are associated with the knowledge of the expected width of the lane. Then, associated lines are fused to a resulting lane, described by the center line and a lane width.

At the end, the lane coefficients are filtered with a low-pass filter.

In the following, some details and some post-processing steps will be presented.

### 2.2 Line Association

The various line sources may have different points of expansion, starting points and validity ranges. Therefore, before association of sensor lines to fusion lines are performed, all lines are expanded at the same point in x-direction. Otherwise the coefficients cannot be compared. There are three reasons that points of expansion may not be equal. Firstly, the prediction of the fusion lines for the ego-motion compensation leads to a shift relatively to the ego coordinate system (COS). Secondly, sensor lines e.g. NDM segments are allowed to have starting points different from zero. Finally, the incoming sensor lines are synchronized to the same fusion time and so they are shifted the same way as the fusion lines. The transformation is carried out in following the three steps: (example given for transforming line 1 from  $x_{01}$  to  $x_{02}$ )

1. Transformation to canonical coefficients:

$$y_1 = y_{01} + \tan(\psi)(x - x_{01}) + \frac{1}{2}c_0(x - x_{01})^2 + \frac{1}{6}c_1(x - x_{01})^3 \quad (2)$$

$$\Updownarrow \text{ with } a_0 = y_{01}, a_1 = \tan(\psi),$$

$$a_2 = \frac{1}{2}c_0, a_3 = \frac{1}{6}c_1$$

$$y_1 = a_0 + a_1(x - x_{01}) + a_2(x - x_{01})^2 + a_3(x - x_{01})^3$$

2. Transformation of the point of expansion from  $x_{01}$  to  $x_{02}$  resulting in new coefficients  $a'$

$$\begin{aligned}
y_1 &= a_0 + a_1(x - x_{02}) + a_2(x - x_{02})^2 \\
&\quad + a_3(x - x_{02})^3 \\
\Downarrow \text{ with } & a_0 = a_0 + a_1(x_{02} - x_{01}) \\
& a_1 = a_1 + 2a_2(x_{02} - x_{01}) \\
& a_2 = a_2 + 3a_3(x_{02} - x_{01}) \\
& a_3 = a_3
\end{aligned} \quad (3)$$

### 3. Retransformation to model description

$$\begin{aligned}
y_1 &= y_{01} + \tan(\psi')(x - x_{02}) + \frac{1}{2}c_0'(x - x_{02})^2 \\
&\quad + \frac{1}{6}c_1'(x - x_{02})^3 \\
\Downarrow \text{ with } & y_{01} = a_0', \psi' = \arctan(a_1') \\
& c_0' = 2a_2', c_1' = 6a_3'
\end{aligned} \quad (4)$$

Hereafter, gate association is carried out: a sensor line is associated to a fusion line if all of the following conditions are satisfied

- the overlap along the x-direction of two lines is bigger than a threshold,
- the lines' distance at the midpoint of the overlap is smaller than an adaptive maximum threshold (adaptivity given by change in curvature)
- the lines' distance at the midpoint of the overlap is bigger than an adaptive minimum threshold (threshold equals zero for association of lines)
- the difference of  $\psi$  is smaller than a threshold,
- the difference of the curvature is smaller than an adaptive limit (adaptivity depending on the curvature of the lines)

An input line not associated creates a new pre-fusion line.

### 2.3 Lane building

After calculating the resulting pre-fusion lines lane building takes place under the following basic assumptions:

1. Lane segments are parallel
2. The lane width is confined by a min and max value
3. Each line contributes to at least one lane
4. At least one ego lane exists as long as any line has been detected.

Association of lines to lanes is carried out using the same method described in section 2.2. A different parameter set for the threshold values is chosen and multiple assignments of a line are allowed.

Lines which have not found a partner line for a lane are treated separately. To these remaining lines one or two parallel shifted partner lines are guessed resulting in one or two lanes. The decision if one or two lines are guessed depend on the starting point and orientation of the line with respect to the ego vehicle. The value of the lateral shift is taken from a memory of recent lane widths. Guessed lines will be deleted during the split process at

the beginning of a fusion cycle. Some examples of lane building are illustrated in Fig. 3.

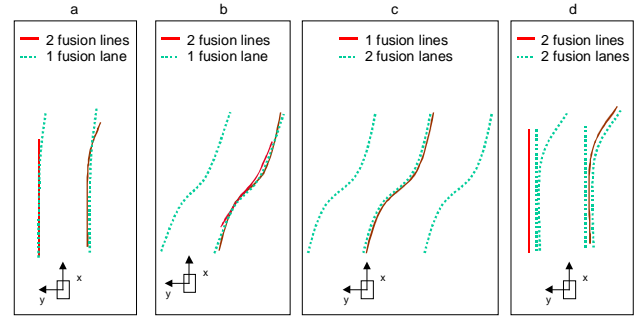


Fig. 3: Four examples for lane building from fusion lines. a) standard case b) one guessed lane due to obvious position of fusion lines with respect to ego vehicle c) two guessed lanes due to unresolved situation d) two guessed lanes due to not associated fusion lines

### 2.4 Determination of lane category

After lane building an ACC function specific lane attribute is determined: the lane category, i.e. the assignment of the lanes into the ego lane and neighboring lanes. The categorization is based on the relative position, orientation, and velocity of the ego vehicle and is a predictive approach in order to determine a new ego lane early. So, even if the fraction of the ego vehicle's outer dimension is physically in one lane and the orientation between the ego vehicle and the lane is bigger than a limit (e.g. ego lane change), a neighboring lane may be assigned as ego lane. The limit depends on velocity in order to represent the drivers typical behavior to cut out softer at higher velocities. One possible result is that more than one lane may be determined as ego lane. This, in turn, will be interpreted by the ACC function as a possible course hypotheses. The final decision for one of these hypothesis will be made by comparison with the yaw rate based course and the overall control strategy followed.

An additional request is, that if at least one line is detected, an ego lane must be given to the function. Therefore, a special post-processing even produces a lane with two guessed lines only based e.g. on the outer line from a neighboring lane. This and other examples can be seen in Fig. 4.

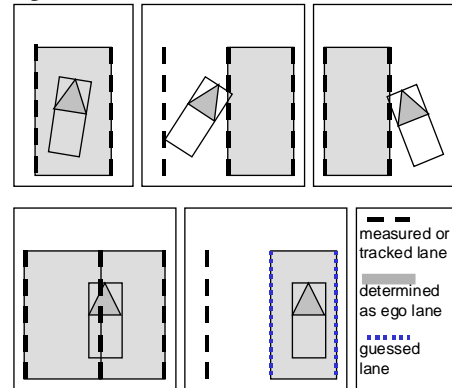


Fig. 4: Five examples for lane categorization.

## 2.5 Results for coefficient fusion

For each type of line source special assumption and heuristics need to be incorporated in the fusion process. In the example shown here the LDF of video lines (VL) and trajectory lines derived from moving objects (MOL) are discussed. Furthermore, an example is shown where curvature data retrieved from navigation-digital map (NDM) is incorporated in the LDF.

The basic assumption for using trajectories of moving objects as source of lane information is that vehicles move within lanes. The path a vehicle in front of the own vehicle has taken is a potential path the ego vehicle must also follow. However, due to this assumption special care must be taken to select and pre-process trajectories, e.g. a gating mechanism to select trajectories must be applied for robust fusion (e.g. cut-ins violate the assumption and are disregarded – they can be recognized by searching interception points between a fusion line and a trajectory). The lateral offset of the trajectory is also a parameter which calls for special treatment due to fluctuations in the lateral position of the measured data constituting a fusion object and due to the unknown position of the object with respect to the lane in reality. However, often the best guess is that vehicles move on average in the center of a lane. Therefore, the lateral position is another parameter to be considered in the gating mechanism to allow only nearest neighbors trajectories of the fusion line to be considered.

MOL data is modeled using the same polynomial than equ. (1) and applying a sequential Kalman filter approach. The coefficients are estimated based on spatial position of the objects within a temporal history of 5-10s sampled at approx. 0.1s. Measures of quality for the coefficients are derived. Trajectories may be regarded as valid once the ego vehicle has passed a historical longitudinal position of the objects trajectory for the first time or if either the history or the calculated confidence are above a threshold value.

Fig. 5 and Fig. 6 give examples of the LDF results combining VL and MOL information by means of weighted average of the corresponding polynomial coefficients. The minimum lane width parameter for the lane association is set to 2.5m in the example.

In cases the curvature and changes in curvature are not too big the coefficient based LDF has proven to be more robust than expected when viewed in spatial coordinates. It seems to us that performing coefficient based LDF is quite suitable, if consequent pre-selection of lines is applied, the constraints to the model parameter are well adjusted and if the  $c0$  and  $c1$  value are confined.

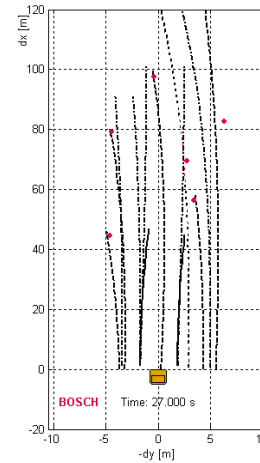


Fig. 5: LDF (dashed-dotted) between VL (solid) and MOL (dashed) without gating/pre-selection. (dots: fusion objects, minimum allowed lane width in lane-association 2.5m)

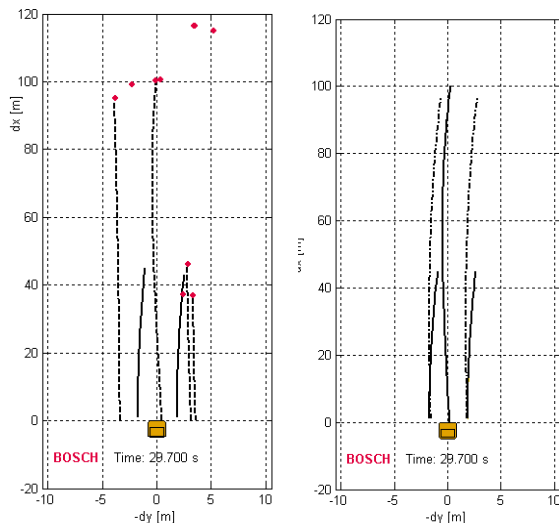


Fig. 6.: Left: Estimated VL (solid) and MOL (dashed) (dots: fusion objects). Right: LDF (dashed-dotted) with gating/pre-selection.

For the integration of NDM data, the LDF representation is divided into three segments. The first segment is dominated by VL, the second by MOL and the third by NDM. This hierarchy accounts for the typical relative accuracy of the different information sources. Segments are, again, modelled according to equ. (1). Segment borders are chosen according to the actual detection range of the dominant lane source within a segment. To this end segmentation of input line information (MOL and NDM) as well as fusion lines/lanes from the previous cycle must be adjusted and coefficients recalculated to the changing segment lengths at the beginning of a new LDF cycle. Association between MOL and VL is carried out in the first segment and is inherited to the second segment. NDM data is retrieved from shape points of a road layout rather than from a lane layout. Therefore, it is less accurate than VL and MOL for the purpose of LDF

discussed in this paper. In addition, the NDM is not synchronised with the other sensors, resulting in a substantial and variable time delay (up to approx. 2.5s). Therefore, for the third NDM dominated LDF segment just the curvature and change of curvature of NDM data is used at the position at which the best curvature match between the second segment and the NDM data is achieved.

Continuity of  $dy$  and  $\psi$  is enforced by onward propagation of the data to the transition of adjacent segments.

Fig. 7 shows a comparison between the curvature in the first segment of NDM and LDF respectively. As reference the yawrate/ $v_{ego}$  representing the curvature of the course of the ego vehicle is also shown. The time delay of the NDM data can be seen.

In the top views of Fig. 8 the LDF results using VL, MOL and NDM as line input data are shown at two different points in time. Also shown is the course the ego vehicle has actually taken.

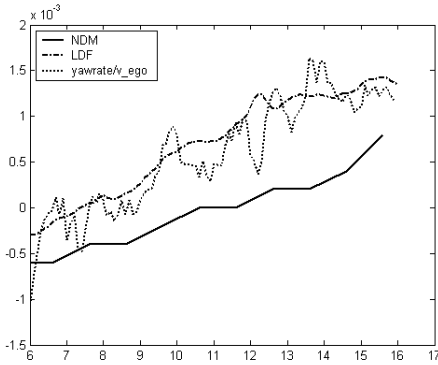


Fig. 7.: Comparison between the curvature given by LDF (dash-dotted), the first segment of NDM (solid) and the ego vehicle course derived by the yaw rate divided by ego velocity (dotted).

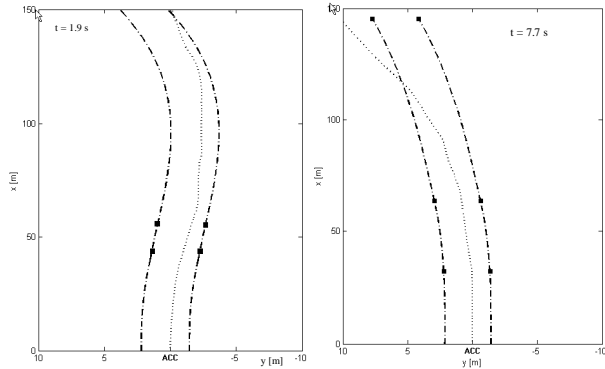


Fig. 8.: Top view of LDF with three segments (dashed-dotted, segment borders indicated by squares) at two different times compared to the actually driven course of ego vehicle (dotted).

### 3 Lane data fusion in spatial coordinates

The algorithm for the fusion of line model coefficients assumes that the coefficients of the different line input data are comparable and similar and so can be fused by

weighted averaging. But, in general, it is not guaranteed that the different line models may lead to coefficients being comparable. And even if the models are equal the coefficients of different input sources may not be similar in coefficient space although they are similar in spatial coordinates. Another potential source of erroneous or unstable behavior of coefficient fusion may occur if lines with different length or different overlap are fused without care. It is not intrinsically guaranteed that the weighted coefficient averaging will lead to a result similar to the input data, because extrapolation is not allowed beyond the defined range of the model description. This will become worse the higher the order of the applied line model. Therefore, theoretically, the coefficient based approach tend to a lack of robustness.

As solution for these potential problems the fusion of line data in spatial coordinates has been proposed, e.g. in [6]. In order to analyze the properties of a LDF in spatial coordinates the key fusion functionalities are implemented and tested. The methods and results are shown in the following.

The underlying representation of the lines are 2D points relative to the ego-vehicle-COS, which are equidistantly sampled along the x-axis, starting at  $x=0$ . As input and output interface of the LDF a coefficient representation is chosen in order to reduce the necessary data rates.

The main fusion steps are similar to the coefficient fusion (Fig. 2). Major difference is the data representation in each step and a slightly different order of split and prediction steps.

The association is done by calculating a weighted mean distance value between related pairs of points of the sensor line and the fusion line in the overlapping part of the lines. This value is compared with an association gate. Weighting of the distance between a pair over the longitudinal distance can be used to introduce the knowledge about the sensor model, e.g. the decreasing confidence of video lines with increasing distance. Fig. 9 shows the principle of the association.

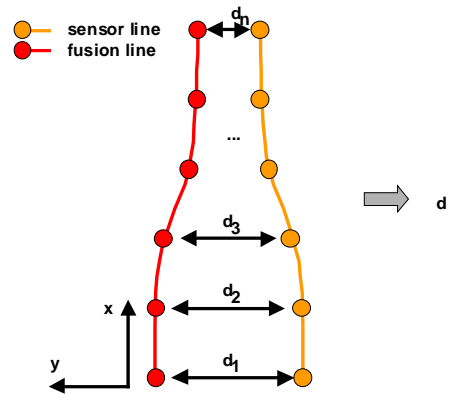


Fig. 9: Principle of the association process in spatial coordinates.

The calculation follows eq. (4):

$$d = \sum_{i=1}^n w_i d_i \quad w_i : \text{normalized weights}, d_i : \text{pair dist} \quad (4)$$

The fusion (‘measurement update’) of an associated set of data points is performed in two steps. First, ‘pre-fusion’ points are calculated from all points associated to a sequence of fusion points from the previous cycle by a weighted mean. Hereafter, the measurement update and transformation to coefficient representation is done by fitting a polynomial line model using a least squares method, for details see the discussion of the results in the next section.

### 3.1 Results for spatial and coefficient LDF

The resulting pre-fusion set of data points is determined by weighted averaging of all points of associated lines for each sampled distance. The weights, again, are used to introduce knowledge about the uncertainties of the input data or to define the lines convergence behavior beyond the overlapping areas. In the non-overlap area it is not suitable to take only the points of the longer line (black dots), because the influence of these few points on the following coefficients estimation is disproportional to the other points and will lead to an unstable or oscillating behavior of the LDF result. To achieve a better behavior, a heuristic is used to reach better convergence. This is done by filtering the complete sequence of the pre-fused points with a low-pass (Fig. 10). A similar performance is expected if outliers are present.

In a next step, the filtered pre-fused points are used to estimate the coefficients of a third-degree polynomial model (Fig. 11), equ. (1). The estimation is performed by an iterative least squares method. A Kalman-filter with sequential innovation may be used alternatively. The result can be filtered easily by a low-pass filter or simultaneously with the coefficient estimation in the Kalman-filter.

The following two figures show the comparison of the coefficient and spatial LDF results in the case of two simulated input lines of similar (Fig. 10) and different (Fig. 11) lengths. The examples are to highlight some of the problems which might arise for the relevant data sources of LDF discussed in this paper. Data points retrieved from MOL and NDM are not very well compatible under the objective to model lanes. All information is carried in the 2D space and not in the four dimensional coefficient space discussed before. Therefore, pre-selection of compatible or “allowed” data points for spatial LDF seems even more critical than for coefficient fusion.

The sensitivity of the spatial LDF to single data points is shown Fig. 10. The spatial LDF performance is very much dominated by the last data point of the longer line and tend to unstable behavior. This can be reduced by the previously mentioned low pass filtering of the pre-fused points. If there are more remaining data points of the longer line the effects are still present, but reduced though (Fig. 11). In the examples coefficient fusion delivers a more stable output. However, when the difference in length of the input lines become larger the coefficient fused line does not follow the input line very well. A way to overcome this by means of segmentation has been discussed in the previous section.

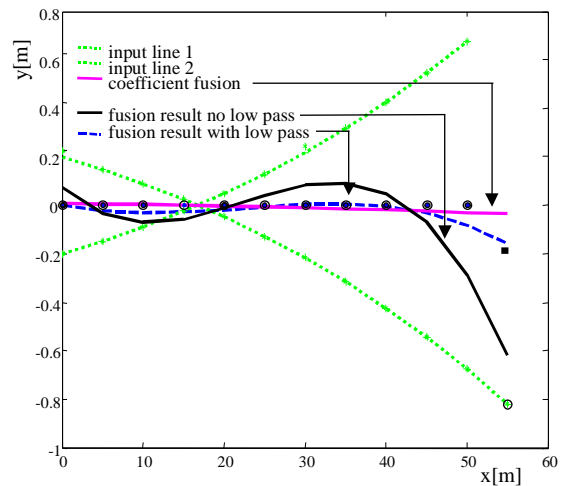


Fig. 10: Comparison of coefficient fusion and spatial fusion with and without low pass filter on data points for two input lines of similar length.

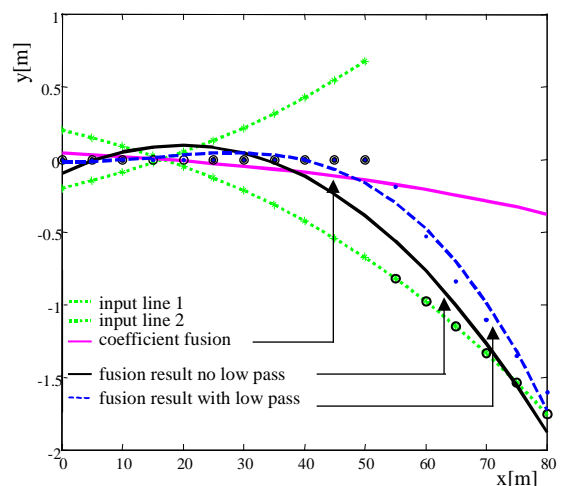


Fig. 11: Comparison of coefficient fusion and spatial fusion with and without low pass filter on data points for two input lines of different length.

## 4 Summary and conclusion

Algorithms for lane data fusion (LDF) for ACC applications have been investigated. Different sources of information have been considered, namely lane markings detected by a video sensor, trajectories from moving objects and data retrieved from a digital map. Approaches for coefficient fusion and fusion in spatial coordinates have been discussed and first results presented.

The coefficient fusion has proven more robust than expected for well conditioned input lines. One reason for this is that the four dimensional coefficient space introduces a greater freedom to account for a priori known properties of the data sources under consideration compared to the 2D space in spatial LDF. It was found that pre-selection of adequate input lines and segmentation solve some of the inherent problems associated to coefficient fusion.

## 5 References

- [1] H. Winner, Die lange Entwicklung von ACC, in *Fahrerassistenz-Workshop*, Leinsweiler, Germany, Sept. 22-24 2003
- [2] F. Paetzold, U. Franke and W. v. Seelen, Lane recognition in urban environment using optimal control theory, *Proc. IEEE Intelligent Vehicles Symposium*, Dearborn, USA, Oct. 3-5 2000, 221-226
- [3] J. Goldbeck and B. Hürtgen, lane detection and tracking by video sensors, *IEEE Proc. Conf. on Intelligent Transportation Systems*, Tokyo Japan, Oct. 5-8 1999
- [4] J. Sparbert, K. Dietmayer, D. Streller, Lane Detection and Street Type Classification using Laser Range Images, *IEEE Conf. on Intelligent Transportation Systems*, Sydney, Australia, Aug. 2001
- [5] E. Dickmanns and A. Zapp, A curvature-based scheme for improving vehicle guidance by computer vision, *Proc. SPIE Conference on Mobile Robots*, vol. 727, 1986
- [6] D. Schwartz, clothoid road geometry unsuitable for sensor fusion, in *Proc. IEEE Intelligent Vehicle Symposium*, Columbus, Ohio, June 9-11 2003, pp. 484-488